
Deep Neural Networks with Auxiliary-Model Regulated Gating for Resilient Multi-Modal Sensor Fusion

Chenye Zhao¹ Myung Seok Shim¹ Yang Li¹ Xuchong Zhang² Peng Li¹

Abstract

Deep neural networks allow for fusion of high-level features from multiple modalities and have become a promising end-to-end solution for multi-modal sensor fusion. While the recently proposed gating architectures improve the conventional fusion mechanisms employed in CNNs, these models are not always resilient particularly under the presence of sensor failures. This paper shows that the existing gating architectures fail to robustly learn the fusion weights that critically gate different modalities, leading to the issue of fusion weight inconsistency. We propose a new gating architecture by incorporating an auxiliary model to regularize the main model such that the fusion weight for each sensory modality can be robustly learned. As a result, this new auxiliary-model regulated architecture and its variants outperform the existing non-gating and gating fusion architectures under both clean and corrupted sensory inputs resulted from sensor failures. The obtained performance gains are rather significant in the latter case.

1. Introduction

Sensor fusion is key to many applications such as autonomous systems equipped with multiple sensing modalities. For instance, cameras and LIDARs are combined to allow image recognition with deep neural networks (Girshick, 2015; Jain et al., 2016; Bohez et al., 2017; Ku et al., 2017; Chen et al., 2017; Wei et al., 2018; Patel et al., 2017; Garcia et al., 2017; Karpathy et al., 2014; Mees et al., 2016). Inertial measurement units (IMUs) and other sensors are utilized in portable devices, e.g. smartphones and smartwatches, for activity recognition. Various sensor fusion techniques for activity recognition have been proposed (Ordóñez & Roggen,

2016; Dehzangi et al., 2017; Zhao & Zhou, 2017; Gravina et al., 2017; Yurtman & Barshan, 2017). More broadly, (Ramachandram & Taylor, 2017) provides a review of multi-modal fusion in terms of architecture and regularization.

Specifically, (Chen et al., 2017) presents a deep convolutional neural network approach to sensor fusion for autonomous driving, where the KITTI dataset (Geiger et al., 2012) containing LIDAR bird view, LIDAR front view, and RGB images is adopted as a benchmark. Three fusion schemes are compared: early fusion, late fusion, and deep fusion. Early fusion refers to the simple combining of features extracted from different modalities using convolutional layers early in the processing flow. Late fusion blends pre-processed features of different modalities towards the output layer of the network. Deep fusion employs multiple stages of blending and splitting of the processed features from different sensors. However, sensor failures are not considered and no deep insight on the working mechanism of sensor fusion is presented in this work.

It is important to note that a key objective and challenge in sensory fusion is attaining *resilience*, i.e., the fusion task shall be facilitated robustly not only under clean sensory inputs but also in the presence of one or multiple sensor failures, which is the main focus of our research.

The following papers are highly related to our work. (Mees et al., 2016) proposes a fusion architecture of a mixture of deep experts, where combined high-level features are fed to a gating network, which generates weights for all expert classification outputs before generating the final decision. (Patel et al., 2017) proposes a gated convolutional neural network called *NetGated* architecture, where two fusion weights extracted from the camera and LIDAR inputs are used to multiply the corresponding pre-processed camera/LIDAR features, respectively, to compute a weighted sum of the two. The weighted sum passes through fully connected layers to produce final robot steering commands. The gating architecture in (Kim et al., 2018) is similar to the *NetGated* architecture in spirit. A weight map is extracted for each sensory modality from the concatenated multi-sensory feature maps produced at each convolutional processing step, and then the weight map is multiplied with the feature maps of the corresponding modality. These weighted feature maps

¹Department of Electrical and Computer Engineering, Texas A&M University, Texas, USA ²Institute of Artificial Intelligence and Robotics, Xi'an Jiaotong University, Xian, P. R. China. Correspondence : Peng Li <pli@tamu.edu>.

are concatenated and further processed to produce a fused feature map.

When compared with conventional non-gating fusion mechanisms, e.g. ones in (Chen et al., 2017), the above gating architectures demonstrate modestly improved robustness under sensor failures. Non-robustness of these architectures are also visible; there are cases where these gating architectures even underperform more conventional non-gating architectures. While the existing gating architectures show promise, they are limited by the black-box nature of the employed fusion mechanisms, which prevents the development of a deep understanding of the relationship between the integrity of sensory modalities, fusion weights, network architecture, and the resulting performances as well as further performance improvements.

To address the above challenges, we present an optimized gating architecture with improved performance and resilience under clean sensory inputs and sensor failures. Our main contributions are: **1)** propose a new auxiliary-model regulated gating architecture, called *ARGate*, to robustly learn fusion weights for different modalities using auxiliary sensory processing paths; **2)** As part of the *ARGate* architecture, propose three regulation techniques, namely, *weight sharing*, *fusion weight regularization*, and *auxiliary loss weighting* to significantly improve the performance and robustness of sensor fusion under clean and corrupted sensory inputs; and **3)** present in-depth analysis of the *ARGate* architecture and its variants to shed light on the employed fusion and regularization mechanisms that are responsible for the observed performance improvements.

We perform comprehensive evaluation of the proposed *ARGate* architecture and its variants while comparing with a baseline fusion CNN architecture and the NetGated architecture (Patel et al., 2017) utilizing the HAR dataset (Anguita et al., 2013) and CAD-60 dataset (Sung et al., 2012) for human activity recognition under various sensory input conditions. It is demonstrated that the proposed architectures consistently outperform the baseline and NetGated architectures, and improve the classification accuracy by upto 10.02% and 14.6% over the baseline and NetGated architectures, respectively.

2. The NetGated Architecture

In (Patel et al., 2017), the NetGated architecture is proposed for unmanned ground vehicle control using a camera and a LIDAR as illustrated in Fig. 1. Input data from two sensors are processed independently through a set of convolutional/pooling layers (blue), and fully connected (FC) layers (red). The outputs of the FC layers “FC-1” and “FC-2” are concatenated and then fused by another FC layer “FC-con”, where two scalar fusion weights are extracted. The outputs

of “FC-1” and “FC-2” are multiplied with the corresponding fusion weights. Finally, these weighted feature outputs are blended in the last FC layer “FC-out”, which produces the final classification decision.

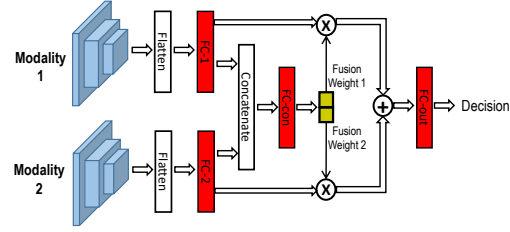


Figure 1. The NetGated architecture (Patel et al., 2017).

2.1. Limitations of the existing gating architectures

The gating architectures such as NetGated extract a fusion weight (map) for each sensory input (Kim et al., 2018; Mees et al., 2016; Patel et al., 2017). Ideally, the fusion weights shall reflect the integrity and importance of the corresponding sensor modality with respect to the classification task. For example, when a particular sensory modality is corrupted by large sensor noise or failures, one would expect to effectively gate off this modality by its small or zero-valued fusion weight.

However, the end-to-end black-box nature of these gating architectures can lead to *fusion weights inconsistency*. We have observed that the fusion weights extracted by the NetGated architectures tend to be unstable and fail to consistently reflect the importance of different modalities. For instance, synthetic datasets are set up such that the sensory modality s_1 is known to be more critical than another modality s_2 for certain classification task. However, the weight for s_1 extracted by the NetGated architecture can actually be lower than that of s_2 . On the other hand, when s_1 is corrupted by sensor failures and therefore has no useful information, its fusion weight can actually be greater than that of s_2 . It is also observed that poor performance may be resulted when fusion weights inconsistency occurs.

3. The Proposed Basic ARGate Architecture

The instability and idiosyncrasies of the existing gating architectures can limit their performance and compromise their resilience with respect to sensory failures. As such, we propose the *ARGate* architecture with internal regulation mechanisms for resilient sensor fusion under clean inputs and in the presence of sensor failures.

We recognize that the key limitation of gating architectures such as NetGated is that the training of feature extractions for different modalities and extraction of fusion weights are blended together in a black-box manner. These two important sub-learning tasks, however, are not optimized individ-

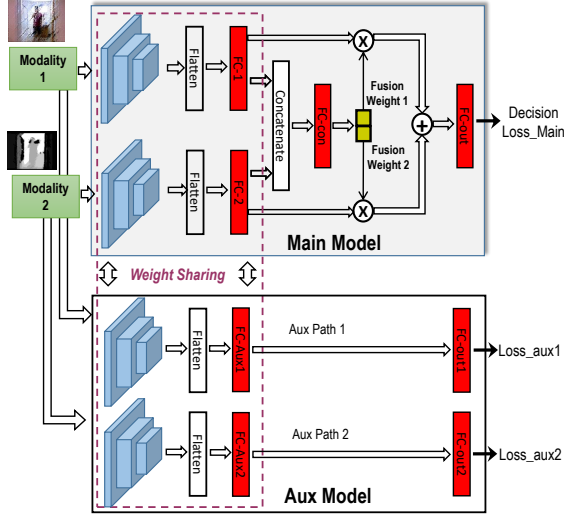


Figure 2. The proposed basic ARGate architecture (ARGate-WS) with an auxiliary model for training. Only the trained main model is employed for inference.

ually to serve their respective purposes. For instance, In the NetGated architecture, the set of convolutional/pooling layers (shown in blue in Fig. 1) are trained together with the portion of the network that does fusion weight computation, particularly the FC layer “FC-con”.

As a first step towards addressing the above issue, we propose the basic ARGate architecture in Fig. 2. To assist the training of the main model, which is employed during the inference phase, an auxiliary (aux) model is included. This architecture can be easily extended to include a greater number of sensory modalities, and additional convolutional/pooling and fully-connected layers may be added to increase the network depth. Architecturally, the main model is almost completely identical to the NetGated architecture. When splitting the output of the “FC-con” layer into the fusion weights, we further introduce L2 normalization and a softmax function to normalize the fusion weights.

The Aux model consists of multiple independent auxiliary paths, one for each modality and without fusion. As illustrated by the dashed purple box in Fig. 2, the weight parameters for the convolutional layers and early FC layers are shared between the corresponding modalities between the main and aux models, which is referred to as *weight sharing* (WS). We dub this basic architecture ARGate-WS. The entire network is trained using the following weighted loss function for K sensors:

$$Loss = \alpha \cdot Loss_{main} + \sum_{k=1}^K Loss_{aux}^k, \quad (1)$$

where $Loss_{main}$ and $Loss_{aux}^k$ are the losses for the main model and the k -th auxiliary path for the same classification

task, respectively, and α is a user-specified weighting factor.

The key idea here is that since the loss of each auxiliary path is included in the overall training loss, the convolutional and early FC layers of the auxiliary path are trained to achieve a good classification performance while using only one sensory modality. Sharing these weights with the corresponding layers in the main model acts as an effective regularization mechanism for the main model, which also forces the “FC-con” layer in the main model to be trained to more robustly learn the fusion weights. We will demonstrate the performance improvements of this basic ARGate model in Section 6.

4. Enhanced Regulations in ARGate

While the basic ARGate architecture (ARGate-WS) offers improved performance, we explore additional regulation techniques as shown in Fig. 3.

4.1. Fusion Weight Regularization (FWR)

When one or more sensory channels are completely corrupted, weight sharing (WS) in ARGate-WS fails to enhance the corresponding convolutional/FC layers for the corrupted input channels in the main model. This is because that these auxiliary paths can no longer be trained to deliver a good performance based on the single corrupted modality.

Our key observation is that the losses of different auxiliary paths reflect the relevance of these modalities w.r.t. to the classification task, and hence, can be used for *fusion weight regularization* (FWR), which is depicted using a purple dashed line pointing from the aux model to the main model in Fig. 3. When a particular sensory modality is corrupted under an input example, the high loss of its auxiliary path will constrain the training of the “FC-con” layer in the main model to produce a low fusion weight for that modality. We realize fusion weight regularization (FWR) by adding an additional term to the training loss:

$$Loss = \alpha \cdot Loss_{main} + \beta \cdot \sum_{k=1}^K Loss_{aux}^k + \sum_{k=1}^K \left(w_{fusion}^k - \frac{e^{-Loss_{aux}^k}}{\sum_{k=1}^K e^{-Loss_{aux}^k}} \right)^2, \quad (2)$$

where β is another user-defined weighting factor, and w_{fusion}^k is the fusion weight for the k -th modality outputted by the “FC-con” layer in the main model. Each normalized auxiliary-path loss $\frac{e^{-Loss_{aux}^k}}{\sum_{k=1}^K e^{-Loss_{aux}^k}}$ is employed to regularize w_{fusion}^k . Here, $e^{-Loss_{aux}^k}$ is obtained by plugging $Loss_{aux}^k$ into the exponential function and then normalizing $e^{-Loss_{aux}^k}$ using L2 and then softmax normalization so that $\frac{e^{-Loss_{aux}^k}}{\sum_{k=1}^K e^{-Loss_{aux}^k}}$ is between [0,1]. The architecture with

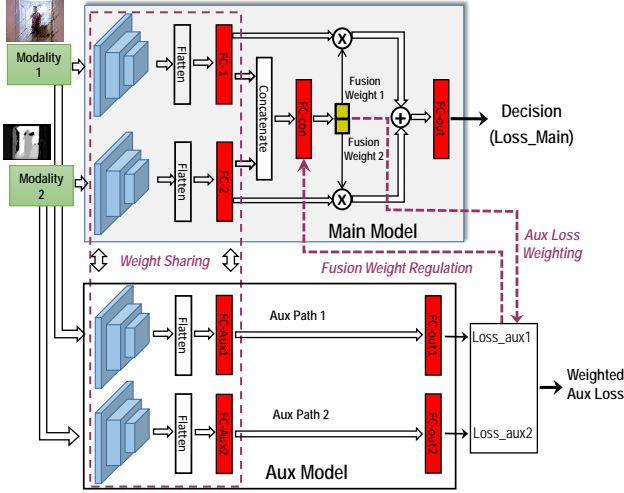


Figure 3. The full ARGate architecture (ARGate-F).

both weight sharing (WS) and fusion weight regularization (FWR) is dubbed ARGate-WS-FWR.

4.2. Auxiliary Loss Weighting (ALW)

Since the loss of each auxiliary path is included in the total loss in (1) or (2), the large loss of any corrupted sensory input can dominate other terms in the loss function, potentially leading to degraded performance. To address this problem, we use the extracted fusion weights from the main model to regularize all auxiliary losses as shown by the dashed purple line pointing from the main model to the aux model in Fig. 3. This leads to the full ARGate architecture (ARGate-F) with a new loss function:

$$Loss = \alpha \cdot Loss_{main} + \beta \cdot \sum_{k=1}^K w_{fusion}^k Loss_{aux}^k + \sum_{k=1}^K \left(w_{fusion}^k - e^{-Loss_{aux}^k} \right)^2, \quad (3)$$

where the auxiliary path loss $Loss_{aux}^k$ is weighted by the fusion weight w_{fusion}^k , hence the dominance of any large auxiliary path loss resulted from sensor failures is reduced.

While ARGate-WS and ARGate-WS-FWR both improve performance, the full ARGate architecture (ARGate-F) with both fusion weight regularization and auxiliary loss weighting consistently produces the best performance, as will be demonstrated.

5. Experimental Settings

We perform comprehensive comparison of a fusion CNN baseline (Chen et al., 2017), the NetGated architecture (Patel et al., 2017), and variants of the proposed ARGate architecture on the HAR (Anguita et al., 2013) and CAD-60 (Sung

et al., 2012) datasets for human activity recognition. The ADAM optimizer is utilized with a learning rate of 0.001. The cross-entropy loss is chosen as the loss for the CNN baseline, the NetGated architecture, and the main model and auxiliary paths of ARGate. All simulations are done on Ubuntu 16.04 with Python 2.7 and Pytorch 0.4.0 (Paszke et al., 2017) using NVIDIA TITAN Xp GPUs.

5.1. Datasets

5.1.1. THE HUMAN ACTIVITY RECOGNITION DATASET

The Human Activity Recognition (HAR) dataset (Anguita et al., 2013) includes six activities to be recognized: walking, walking upstairs, walking downstairs, sitting, standing, and laying. Input signals from an accelerometer and gyroscope are gathered at a rate of 50Hz and 128 readings in a sliding window of 2.56 seconds define the input attributes for one example. From a sensor fusion point of view, for each example, readings from the accelerometer and gyroscope define nine sensory inputs: three-axial total accelerations ($total_acc_x$, $total_acc_y$, $total_acc_z$), three-axial body accelerations ($body_acc_x$, $body_acc_y$, $body_acc_z$), and three-axial angular velocities ($body_gyro_x$, $body_gyro_y$, $body_gyro_z$), where each sensory input contains 128 readings distributed between $[-1, 1]$. There are 7,352 samples for training and 2,947 samples for testing.

5.1.2. THE CAD-60 DATASET

The CAD-60 dataset (Sung et al., 2012) consists of 60 videos captured by a Microsoft Kinect device with an RGB video camera and a depth sensor for recognizing 14 human activities. Each video frame is segmented into an RGB and a depth image, forming one example. The feature extraction code provided by the dataset extracts five input features from the raw RGB and depth images: skeletal, skeletal histogram of oriented gradients (HOG) of the RGB image, RGB HOG, skeletal HOG of the depth image, and depth HOG. To demonstrate sensor fusion, we treat each of the five input features as a sensory input. The ‘‘new person’’ setting of (Sung et al., 2012) is adopted to use the data from three people for training and that from the remaining person for testing.

5.2. Neural Network Configurations

All models are trained using 200 epochs with a batch size of 16 for the HAR dataset and 100 epochs with a batch size of 128 for the CAD-60 dataset.

5.2.1. CONFIGURATIONS FOR THE HAR DATASET

The HAR dataset has 9 input channels (sensors).

CNN Baseline. The CNN baseline has the following layers

to process each sensory input before fusion: $C(16,3,1)$ - P - $FC(256)$ - $FC(256)$, where $C(n,f,s)$ represents a 1-D convolutional layer with n filters of size f and stride s , P indicates a maxpooling layer with a non-overlapping sliding window of size 2, and $FC(n)$ represents a fully-connected layer with n ReLU neurons. After pre-processing all input channels, the outputs from the above structures are fused together using element-wise mean and then passed onto three FC layers $FC(128)$ - $FC(64)$ - $FC(6)$. The classification decision is made at the final FC layer $FC(6)$ with a softmax classifier.

NetGated. Following Fig. 1, feature extraction of each channel is based on a simpler structure: $C(16,3,1)$ - P - $FC(256)$ for fair comparison with the CNN baseline. Then, the extracted features from the FC layers, i.e. FC-1 and FC-2 in in Fig. 1, are then concatenated and connected to a structure of $FC(256)$ - $FC(9)$ for computing the fusion weights, which are further normalized. The normalized fusion weights are multiplied with the outputs from the first set of FC(256) layers, resulting a set of weighted features, which are added and fed to two FC layers $FC(256)$ - $FC(6)$. Instead of having two FC layers before the output layer as in the baseline, only one FC layer $FC(256)$ is used, again for fair comparison.

ARGate. According to Fig. 3, ARGate has additional auxiliary paths. Each auxiliary path shares convolutional and FC layer weights with the corresponding layers in the main model. The outputs from these shared FC layers are further processed by another fully-connected layer $FC(6)$ to produce a classification decision one for each path. In the main model, the pre-processed input features are concatenated and fed to FC layers $FC(256)$ - $FC(9)$ for fusion weight extraction. Different from NetGated, here the weighted features are added and then processed only by a single fully-connected layer FC(6) versus two layers FC(256) and FC(6) in Netgated for fair comparison.

Overall, the CNN baseline, NetGated, and ARGate have 853,424, 847,280, and 829,104 learnable parameters, respectively. Our ARGate models have somewhat fewer tunable parameters, therefore the performance improvements of ARGate demonstrated later are not due to inclusion of more learnable parameters.

5.2.2. CONFIGURATIONS FOR THE CAD-60 DATASET

There are five input channels in the CAD-60 dataset: skeletal features, skeletal HOG features on RGB image, RGB HOG, skeletal HOG features on depth image, and depth HOG.

CNN Baseline. When pre-processing each input channel for feature extraction, we use $C(8,3,1)$ - P - $C(4,3,1)$ - P - $C(600,114,1)$ - $FC(600)$ for the skeletal feature channel while the setups for other channels are: $C(8,3,1)$ - P - $C(4,3,1)$ - P - $C(600,48,1)$ - $FC(600)$ for skeletal HOG on RGB, $C(8,3,1)$ -

$C(4,3,1)$ - $C(600,32,1)$ - $FC(600)$ for RGB HOG, $C(8,3,1)$ - P - $C(4,3,1)$ - P - $C(600,48,1)$ - $FC(600)$ for skeletal HOG on depth, and $C(8,3,1)$ - $C(4,3,1)$ - $C(600,32,1)$ - $FC(600)$ for depth HOG, respectively. Note that the RGB HOG and depth HOG inputs are small in size, maxpooling layers are not employed for them. The outputs from the pre-processing stages are combined using element-wise mean, and are then fed to FC layers $FC(600)$ - $FC(600)$ - $FC(50)$ - $FC(14)$.

NetGated. The feature extractions of different input channels are identical to what are adopted in the CNN baseline. However, instead of performing element-wise mean of the extracted features, these features are concatenated, and then passed onto FC layers $FC(3000)$ - $FC(5)$ to extract fusion weights, which are again normalized. The extracted features from all input channels are weighted by the corresponding normalized fusion weights, then the weighted outputs are added and fed to FC layers $FC(1200)$ - $FC(14)$ for making the final classification decision.

ARGate. In the main model, the same setups used in the CNN baseline are employed for pre-processing the five inputs. The extracted features are concatenated and then passed onto two FC layers $FC(3000)$ - $FC(5)$ to extract fusion weights. Along each auxiliary path, the convolutional and fully-connected layers share weights with the corresponding layers in the main model. Each auxiliary path has two fully-connected layers $FC(200)$ - $FC(14)$ and the size of each FC(200) layer is smaller than the corresponding one in NetGated. Outputs from the FC layers $FC(14)$ create losses for the auxiliary paths to regularize the fusion weights and produce a prediction decision solely based on each input channel.

The number of tunable parameters in the CNN baseline, NetGated, and ARGate are 2,619,136, 2,594,236, and 2,594,236, respectively. For the ARGate architecture and variants, α in (1) is set to be 5.0. In (2) and (3), α is set to $\frac{1}{9}$, and β is fixed to $\frac{5}{9}$.

5.3. Fusion Weight Normalization

In the original NetGated architecture (Patel et al., 2017), the scalar fusion weights are extracted from the FC layer “FC-con” (Fig. 1) without normalization. As a result, the range of the extracted fusion weights is not fully controlled. In this work, we apply fusion weight normalization for both NetGated and the proposed architectures since it provides performance improvements as follows. The fusion weights w_{fusion} outputted by the “FC-con” layer are normalized by L2 and then *softmax* normalization: $w_{fusion,n} = softmax(l_{norm}^2(w_{fusion}))$, where the l_{norm}^2 normalizes fusion weights w_{fusion} to be within $[-1, 1]$, which are then normalized by *softmax* to fall in $[0, 1]$ and sum up to 1.0. As such, each scalar fusion weight can be readily interpreted as a measure of criticality of the

corresponding modality for the fusion task.

5.4. Sensor Failures

Apart from using the original clean data from the HAR and CAD-60 datasets, we introduce sensor failures and set up various training/testing sets to comprehensively compare the robustness and generalization of different architectures.

5.4.1. MODELING OF FAILING SENSORS

All clean scalar inputs are normalized to be within $[-1, 1]$. We use three schemes, namely *zero*, *uniform*, and *Gaussian*, to model a failing sensor by setting the corresponding input values respectively to zero, pure noise following a uniform distribution between -1 and 1 , and pure noise following the Gaussian distribution $\mathcal{N}(0, 1)$.

5.4.2. CORRUPTED EXAMPLES FOR TRAINING/TESTING

For each experiment, we use clean and corrupted examples in both the training and test sets, where in each set $\frac{1}{3}$ of the examples are randomly chosen and kept clean while the remaining ones are corrupted by one or more failing sensors using one of the approaches described below.

[Fixed failing sensor assignment.] This scheme mimics the situation in which a certain number of sensors have failed permanently. Correspondingly, we select $n_{f_{clean}}$ channels out of a total of n sensors to be clean and assume that all remaining sensors have permanent failure when setting up the corrupted examples of for both the training and test sets in each experiment.

[Random failing sensor assignment.] Different from the previous scheme, here we attempt to more closely mimic random nature of sensor failures. For each corrupted example in either the training or test set, we randomly select $n_{r_{clean}}$ channels out of all n sensors to be clean and corrupt the remaining channels. As such, sensors that have failed may vary from one example to another.

$n_{f_{clean}}$ and $n_{r_{clean}}$ are varied to introduce different severity levels of sensor failures.

[Failing sensor assignment for model generalization.] This scheme aims to test the generalization of each model by using a test set containing corrupted examples which have a larger or different number of failing sensors from the corrupted examples used to train the model. In other words, the test set has examples with a higher severity level of sensor failure.

6. Evaluation

6.1. Quality of Fusion Weight Extraction

To shed some light on the fusion mechanisms of the NetGated and the proposed ARGate-WS and ARGate-F architectures, we examine the distributions of the learned fusion weight of the sensory input $total_acc_y$ under the HAR dataset after training. The sensor failures are modeled using the random failing sensor assignment with uniform distribution and with $n_{r_{clean}} = 1$ so that eight out of nine sensory inputs are corrupted in each example. To show the effects of sensor failures on fusion weights, we split the examples into two subsets: one in which $total_acc_y$ is corrupted with seven other inputs and the other subset where $total_acc_y$ is the only clean input. Fig. 4(a, b, c) displays the fusion weight distributions of the first subset for the three architectures while Fig. 4(d, e, f) shows those of the second subset.

One may expect that, in a properly trained model, the fusion weight value for a corrupted sensory modality shall be much smaller than when the modality is clean. However even when $total_acc_y$ is corrupted, Fig. 4(a, b, c) show that the $total_acc_y$ fusion weight distribution of the NetGated architecture has a peak around the large value of 0.4 which is not presented in the case of ARGate-WS. The distribution of ARGate-WS has a much reduced mass on large fusion weight values compared to that of the NetGated. Furthermore, the fusion weight value can go beyond 0.4 in NetGated and ARGate-WS while it is pretty much constrained between 0.06 and 0.1 in ARGate-F. One also expect that the fusion weight of $total_acc_y$ shall be large for the second subset since $total_acc_y$ is the only clean input. However, as seen in Fig. 4d, the distribution of NetGated has a large population mass on low fusion weight values. The population mass on low fusion weight values gets reduced significantly in the case of ARGate-WS (Fig. 4e), which is further reduced in ARGate-F for which most fusion weights are distributed between 0.33 and 0.45 as shown in Fig. 4f.

Under this setup, the prediction accuracies of the NetGated, ARGate-WS, and ARGate-F models are 62.90%, 65.69%, and 67.09%, respectively. Based on the weight distributions presented in Fig. 4, we expect that weight sharing (WS) employed in ARGate-WS makes it more robustly learn the quality of each sensory input to achieve a higher accuracy than NetGated. And the inclusion of fusion weight regulation (FWS) and auxiliary loss weighting (ALW) in ARGate-F further improves the learning quality of fusion weights, thereby producing the best classification result among the three architectures.

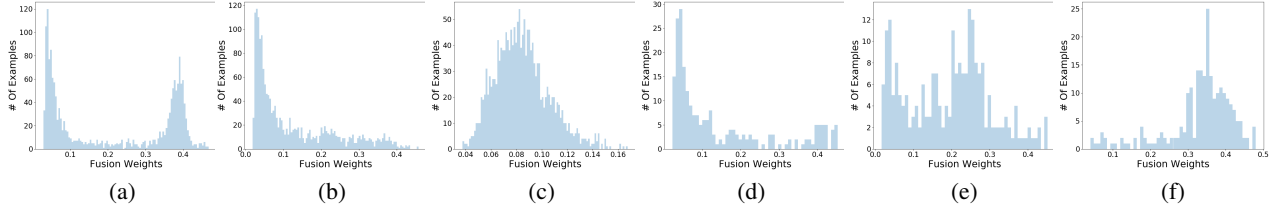


Figure 4. Fusion weight distributions of the clean or corrupted channel total_acc_y extracted by NetGated, ARGate-WS and ARGate-F under random failing sensor assignment with $n_{r\text{clean}} = 1$. (a),(b) and (c) show the fusion weights distributions of the NetGated, ARGate-WS and ARGate-F models, respectively, when total_acc_y is corrupted. (d),(e) and (f) are the distributions of the NetGated, ARGate-WS and ARGate-F models, respectively, when total_acc_y is clean.

Table 1. Prediction accuracies under clean data and random failing sensor assignment for the HAR dataset.

# Clean Channels	Failure Model	Baseline	NetGated	ARGate-WS	ARGate-WS-FWR	ARGate-F
All Clean	-	94.06%	94.50%	94.96%	95.09%	95.69%
$n_{r\text{clean}}=8$	Zero	93.02%	93.17%	94.66%	94.04%	94.60%
	Uniform	92.35%	92.20%	92.45%	92.46%	92.57%
	Gaussian	92.94%	93.28%	94.97%	94.35%	94.13%
$n_{r\text{clean}}=5$	Zero	88.36%	87.95%	88.63%	88.83%	89.89%
	Uniform	86.73%	86.80%	88.53%	89.17%	89.51%
	Gaussian	88.41%	89.04%	89.52%	90.07%	90.12%
$n_{r\text{clean}}=1$	Zero	71.56%	71.12%	74.38%	74.44%	74.62%
	Uniform	62.06%	62.90%	65.69%	66.09%	67.09%
	Gaussian	69.67%	70.54%	71.83%	72.58%	73.19%

Table 2. Prediction accuracies under fixed failing sensor assignment for the HAR dataset.

# Clean Channels	Baseline	NetGated	ARGate-F
$n_{f\text{clean}}=5$	87.68%	89.28%	91.01%
$n_{f\text{clean}}=6$	80.59%	81.94%	84.52%

6.2. Results on the HAR Dataset

[Fixed Failing Sensor Assignment] Based on the fixed failing sensor assignment in Section 5.4.2, we consider two cases where the number of clean input channels $n_{f\text{clean}}$ is set to 5 and 6, respectively. When $n_{f\text{clean}} = 5$, body_total_acc_x , body_acc_x and body_gyro_x are corrupted and set to uniformly distributed noise while body_acc_z and body_gyro_z are corrupted by uniformly distributed noise when $n_{f\text{clean}} = 6$. Three architectures are compared in Table 2, which shows that our proposed ARGate-F outperforms the CNN baseline and NetGated.

[Random Failing Sensor Assignment] In Table 1, we perform comprehensive comparisons between the baseline CNN, NetGated, proposed ARGate-WS, ARGate-WS-FWR, and ARGate-F architectures under random failing sensor assignment with the number of randomly chosen clean sensors $n_{r\text{clean}} \in \{1, 5, 8\}$. When all channels are clean, NetGated has 0.44% prediction accuracy improve-

ment over the baseline while ARGate-WS, ARGate-WS-FWR, and ARGate-F outperform the baseline by 0.90%, 1.03% and 1.63%, respectively. ARGate-WS always has better performance than the baseline and NetGated, and in general ARGate-WS-FWR further improves over ARGate-WS which only employs weight sharing (WS) between the main and auxiliary model, demonstrating the effectiveness of fusion weight regularization (FWR). Overall, ARGate-F is the best-performing model, which incorporates WS, FWR, and ALW (Aux Loss Weighting) (Fig. 3). In particular, when $n_{\text{clean}} = 1$ and sensor failures are modeled using uniformly distributed noise, ARGate-F outperforms the baseline, Netgated, ARGate-WS, and ARGate-WS-FWR by 5.03%, 4.19%, 1.4%, and 1.0%, respectively.

Table 3. Prediction accuracies under failing sensor assignment for testing generalization for the HAR dataset.

# Failing Channels	Baseline	NetGated	ARGate-F
(1,2)(3,8)	72.91%	72.75%	77.10%
(1,3)(4,8)	70.98%	70.78%	75.43%
(1,4)(5,8)	69.38%	69.53%	73.06%

[Failing Sensor Assignment for Model Generalization] We compare different models under failing sensor assignment for model generalization in Section 5.4.2 in Table 3, where the first column specifies the numbers of randomly

Table 4. Prediction accuracies under clean data and random failing sensor assignment for the CAD-60 dataset.

# Clean Channels	Failure Model	Baseline	NetGated	ARGate-WS	ARGate-WS-FWR	ARGate-F
All Clean	-	87.01%	86.57%	87.15%	87.37%	87.51%
$n_{r\text{clean}}=4$	Zero	71.91%	68.87%	75.01%	78.67%	82.01%
	Uniform	69.76%	65.13%	75.07%	78.81%	79.78%
	Gaussian	71.55%	73.81%	73.91%	75.74%	77.93%
$n_{r\text{clean}}=3$	Zero	72.91%	65.48%	71.93%	71.47%	77.13%
	Uniform	69.38%	67.61%	72.58%	71.96%	73.86%
	Gaussian	71.62%	68.83%	71.34%	72.17%	74.75%
$n_{r\text{clean}}=2$	Zero	67.94%	67.98%	65.18%	64.41%	68.17%
	Uniform	64.98%	62.98%	66.07%	66.59%	66.70%
	Gaussian	67.41%	66.55%	64.62%	66.96%	68.51%
$n_{r\text{clean}}=1$	Zero	59.07%	58.18%	57.43%	59.89%	60.01%
	Uniform	61.42%	57.10%	60.10%	61.35%	61.82%
	Gaussian	57.44%	57.75%	57.39%	57.55%	57.96%

Table 5. Prediction accuracies under fixed failing sensor assignment for the CAD-60 dataset.

# Clean Channels	Baseline	NetGated	ARGate-F
$n_{f\text{clean}}=1$	60.60 %	59.98 %	65.14 %
$n_{f\text{clean}}=4$	64.15 %	61.72 %	72.74 %

chosen failing channels used in the training and test sets. For example, (1,2)(3,8) means that the number of failing sensors for training are randomly picked from [1,2] while the range of the failing sensors for testing is [3,8]. Essentially, we evaluate the generalization of the models by including corrupted examples with more failing channels in the test set than in the training set. Failing sensors are modeled using uniformly distributed noise. As can be seen, NetGated can produce a performance even lower than that of the baseline while ARGate-F always outperforms the other two. ARGate-F outperforms the baseline and NetGated by upto 4.45% and 4.65%, respectively.

6.3. Results on the CAD-60 Dataset

[Fixed Failing Sensor Assignment] The comparisons based on fixed failing sensor assignment are shown in Table 5, where the corrupted inputs are set to uniformly distributed noise. When $n_{f\text{clean}} = 1$, skeletal features, RGB HOG, skeletal HOG features on Depth Image, and Depth HOG are corrupted. When $n_{f\text{clean}} = 4$, only the skeletal channel is corrupted. NetGated is in fact worse than the baseline under both settings while ARGate-F significantly outperforms the other two models. For example, when $n_{f\text{clean}} = 4$, ARGate-F improves over the baseline and NetGated by 8.59% and 11.02%, respectively.

[Random Failing Sensor Assignment] In Table 4, different models with the number of randomly selected clean channels $n_{r\text{clean}} \in \{1, 2, 3, 4\}$ are compared. When all five

input channels are clean, NetGated performs worse than the baseline and the proposed ARGate-F improves the baseline and NetGated by 0.5% and 0.94%, respectively. ARGate-F improves over ARGate-WS and ARGate-WS-FWR by 0.36% and 0.14%, respectively. Across different settings, in many cases, NetGated produce a performance noticeably lower than the baseline. ARGate-WS and ARGate-WS-FWR outperform both the baseline and NetGated in most cases. ARGate-F always has the best performance among all models. For example, with $n_{\text{clean}} = 4$ and the uniform noise sensor failure model, ARGate-F significantly outperforms the baseline and NetGated by 10.02% and 14.65%, respectively.

Table 6. Prediction accuracies under failing sensor assignment for model generalization for the CAD-60 dataset

# Failing Channels	Baseline	NetGated	ARGate-F
(1,4)(1,4)	64.08%	63.71%	68.36 %
(2,3)(2,4)	55.36%	55.16%	58.04%
(2,4)(1,4)	60.77%	61.05%	62.19 %

[Failing sensor assignment for model generalization] We specifically compare the generalization of three models in Table 6 where the same notation of Fig. 1 is used. Again, it is observed that NetGated can underperform the baseline while the proposed ARGate-F demonstrates noticeable improvements over the other two models.

7. Conclusion

We have proposed the ARGate architecture and its variants for resilient sensor fusion by addressing the limitations of the conventional fusion schemes including the existing gating architectures. Our architectures have demonstrated significant performance improvements over other models par-

ticularly in the presence of sensor failures. Our future work will demonstrate the application of the ARGate architectures to fusion of more complex sensory modalities such as LIDARs.

References

- Anguita, D., Ghio, A., Oneto, L., Parra, X., and Reyes-Ortiz, J. L. A public domain dataset for human activity recognition using smartphones. In *ESANN*, 2013.
- Bohez, S., Verbelen, T., De Coninck, E., Vankeirsbilck, B., Simoens, P., and Dhoedt, B. Sensor fusion for robot control through deep reinforcement learning. In *Intelligent Robots and Systems (IROS), 2017 IEEE/RSJ International Conference on*, pp. 2365–2370. Ieee, 2017.
- Chen, X., Ma, H., Wan, J., Li, B., and Xia, T. Multi-view 3d object detection network for autonomous driving. In *IEEE CVPR*, volume 1, pp. 3, 2017.
- Dehzangi, O., Taherisadr, M., and ChagalVala, R. Imu-based gait recognition using convolutional neural networks and multi-sensor fusion. *Sensors*, 17(12):2735, 2017.
- Garcia, F., Martin, D., De La Escalera, A., and Armingol, J. M. Sensor fusion methodology for vehicle detection. *IEEE Intelligent Transportation Systems Magazine*, 9(1): 123–133, 2017.
- Geiger, A., Lenz, P., and Urtasun, R. Are we ready for autonomous driving? the kitti vision benchmark suite. In *Conference on Computer Vision and Pattern Recognition (CVPR)*, 2012.
- Girshick, R. Fast r-cnn. In *Proceedings of the IEEE international conference on computer vision*, pp. 1440–1448, 2015.
- Gravina, R., Alinia, P., Ghasemzadeh, H., and Fortino, G. Multi-sensor fusion in body sensor networks: State-of-the-art and research challenges. *Information Fusion*, 35: 68–80, 2017.
- Jain, A., Koppula, H. S., Soh, S., Raghavan, B., Singh, A., and Saxena, A. Brain4cars: Car that knows before you do via sensory-fusion deep learning architecture. *arXiv preprint arXiv:1601.00740*, 2016.
- Karpathy, A., Toderici, G., Shetty, S., Leung, T., Sukthankar, R., and Fei-Fei, L. Large-scale video classification with convolutional neural networks. In *Proceedings of the IEEE conference on Computer Vision and Pattern Recognition*, pp. 1725–1732, 2014.
- Kim, J., Koh, J., Kim, Y., Choi, J., Hwang, Y., and Choi, J. W. Robust deep multi-modal learning based on gated information fusion network. *arXiv preprint arXiv:1807.06233*, 2018.
- Ku, J., Mozifian, M., Lee, J., Harakeh, A., and Waslander, S. Joint 3d proposal generation and object detection from view aggregation. *arXiv preprint arXiv:1712.02294*, 2017.
- Langley, P. Crafting papers on machine learning. In Langley, P. (ed.), *Proceedings of the 17th International Conference on Machine Learning (ICML 2000)*, pp. 1207–1216, Stanford, CA, 2000. Morgan Kaufmann.
- Mees, O., Eitel, A., and Burgard, W. Choosing smartly: Adaptive multimodal fusion for object detection in changing environments. In *Intelligent Robots and Systems (IROS), 2016 IEEE/RSJ International Conference on*, pp. 151–156. IEEE, 2016.
- Ordóñez, F. J. and Roggen, D. Deep convolutional and lstm recurrent neural networks for multimodal wearable activity recognition. *Sensors*, 16(1):115, 2016.
- Paszke, A., Gross, S., Chintala, S., Chanan, G., Yang, E., DeVito, Z., Lin, Z., Desmaison, A., Antiga, L., and Lerer, A. Automatic differentiation in pytorch. In *NIPS-W*, 2017.
- Patel, N., Choromanska, A., Krishnamurthy, P., and Khorrami, F. Sensor modality fusion with cnns for ugv autonomous driving in indoor environments. In *International Conference on Intelligent Robots and Systems (IROS)*. IEEE, 2017.
- Ramachandram, D. and Taylor, G. W. Deep multimodal learning: A survey on recent advances and trends. *IEEE Signal Processing Magazine*, 34(6):96–108, 2017.
- Sung, J., Ponce, C., Selman, B., and Saxena, A. Unstructured human activity detection from rgb-d images. In *Robotics and Automation (ICRA), 2012 IEEE International Conference on*, pp. 842–849. IEEE, 2012.
- Wei, P., Cagle, L., Reza, T., Ball, J., and Gafford, J. Lidar and camera detection fusion in a real-time industrial multi-sensor collision avoidance system. *Electronics*, 7(6):84, 2018.
- Yurtman, A. and Barshan, B. Activity recognition invariant to sensor orientation with wearable motion sensors. *Sensors*, 17(8):1838, 2017.
- Zhao, Y. and Zhou, S. Wearable device-based gait recognition using angle embedded gait dynamic images and a convolutional neural network. *Sensors*, 17(3):478, 2017.